Available online at www.sciencedirect.com

SCIENCE DIRECT®

International Journal of Solids and Structures 42 (2005) 4663–4672

INTERNATIONAL JOURNAL OF SOLIDS and STRUCTURES

www.elsevier.com/locate/ijsolstr

Cantilever beam equilibrium configurations

M. Batista [a,*], F. Kosel [b]

[a] Faculty of Maritime Studies and Transportation, University of Ljubljana, Pot Pomorscakov 4, SI-6320 Portoroz, Slovenia
[b] Faculty of Mechanical Engineering, University of Ljubljana, Askerceva 6, SI-1000 Ljubljana, Slovenia

Received 12 August 2004; received in revised form 8 February 2005
Available online 16 March 2005

Abstract

This article investigates a method for obtaining all equilibrium configurations of a cantilever beam subjected to an end load with a constant angle of inclination. The formulation is based on plane finite-strain beam theory in the elastic domain. An example of a cantilever beam subjected to a horizontal pressure force is discussed in detail.

Keywords: Bifurcation; Cantilever beams; Elastica

1. Introduction

The determination of equilibrium shapes of a cantilever beam subjected to concentrated end loads is one of the oldest problems of elastomechanics. This problem was investigated by Jacob Bernoulli (1705) and later by Leonhard Euler in his treatise on elastic curves (1744) (see, Love, 1944). Assuming that the curvature of the beam is proportional to the bending moment, Euler derived a differential equation for the deformed shape of the beam and solved it with the use of an infinite series. Euler also classified all possible equilibrium states (see, Antman, 1995). Further solutions were obtained by means of elliptic functions and can be found in the relevant literature (e.g., Landau and Lifshitz, 1986; Love, 1944). Recently a method based on a numerical solution of elliptic integrals that enables the determination of all equilibrium configurations at a given load was developed (Navaee and Elling, 1992).

Some authors (Pai and Palazotto, 1996; Saje, 1990, 1991) dealt with the determination of equilibrium configurations considering the final extension and shear strain; however, the aim of these papers was not

* Corresponding author. Tel.: +386 5 6767219; fax: +386 5 6767130.
E-mail address: milan.batista@fpp.edu (M. Batista).

0020-7683/$ - see front matter © 2005 Elsevier Ltd. All rights reserved.
doi:10.1016/j.ijsolstr.2005.02.008

the determination of all configurations, rather just a study of theoretical origins and/or numerical or analytical methods.

The aim of this paper is to propose a relatively simple numerical method, enabling the determination of all equilibrium configurations (shapes) of a cantilever beam with known geometric and material parameters and at a given load.

2. Basic equations

A cantilever beam of length L with constant extension EA, shear GA_s and bending stiffness EI, which is subjected to an inclined constant force $F \geqslant 0$ at its free end, will be discussed (Fig. 1).

The problem will be formulated by means of the finite-strain beam theory (Antman, 1995; Reissner, 1972). According to this theory the deformed state of the discussed beam is defined by the following equations in a non-dimensional form

$$\frac{dx}{ds} = (1+\varepsilon)\cos\varphi - \eta\sin\varphi \quad \frac{dy}{ds} = (1+\varepsilon)\sin\varphi + \eta\cos\varphi \tag{1}$$

$$\frac{d\varphi}{ds} = \kappa \quad \frac{d\kappa}{ds} = -\omega^2\sin\phi\left(1 + v\frac{\omega^2}{\lambda^2}\cos\phi\right) \tag{2}$$

where $s \in [0,1]$ is a parameter, x and y are the coordinates of a point on the beam's axis, $\varphi$is the angle of inclination of the cross-section with respect to y axis, $\phi = \varphi - \alpha$ and κ is the bending strain of the beam. The extension strain ε and the shear strain γ are determined with

$$\varepsilon = -\frac{1}{2}(1-v)\frac{\omega^2}{\lambda^2}\cos\phi \quad \gamma = \frac{1}{2}(1+v)\frac{\omega^2}{\lambda^2}\sin\phi \tag{3}$$

Non-dimensional parameters ω, λ, v used in (2) and (3) are defined as follows

$$\omega^2 = \frac{FL^2}{EI} \quad \frac{1}{\lambda^2} = \frac{1}{\lambda_T^2} + \frac{1}{\lambda_S^2} \quad v = \frac{\lambda_T^2 - \lambda_S^2}{\lambda_T^2 + \lambda_S^2} \tag{4}$$

where $\frac{1}{\lambda_T^2} = \frac{EI}{L^2 EA}$ and $\frac{1}{\lambda_S^2} = \frac{EI}{L^2 GA_s}$. It is seen from (4) that the values of parameter v are restricted to the interval $[-1, 1]$. For $v = -1$ the beam allows no shear strain, while for $v = 1$, it allows no extension strain. It has to be mentioned that the elastica is not defined by the condition $v = 0$, but by $1/\lambda = 0$.

Eqs. (1) and (2) can be solved together with boundary conditions. In the discussed case the boundary conditions have the following form

$$x(0) = y(0) = 0 \tag{5}$$

$$\phi(0) = -\alpha \quad \kappa(1) = 0 \tag{6}$$

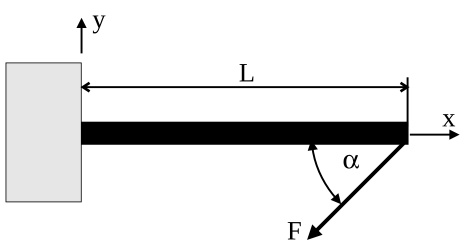

Fig. 1. Undeformed state of a cantilever beam.

Because of the fact that a portion of the beam cannot be deformed into a single point and the shear strain cannot have such values that could lead to overlapping of the cross-sections and the axis of the beam, it has to be stressed that ε is limited by $1+\varepsilon > 0$. Together with the first expression of (3), this restriction implies

$$\frac{\omega}{\lambda} < \sqrt{\frac{2}{(1-v)|\cos\phi_{\min}|}} \tag{7}$$

where $\phi_{\min} = \min\hat{\phi}(s),\ s\in[0,1]$.

3. Solution

The form of Eqs. (1) and (2) and boundary conditions (5) and (6) suggests that Eq. (2), which have to fulfil the conditions (6), can be solved independently of Eq. (1). The second set of boundary conditions (6) defines a two-pointed boundary problem, which can be solved by means of Picard's shooting method (Antman, 1995; Ascher et al., 1995; Forsythe et al., 1977). The idea of the method is the following: consider $\kappa = \hat{\kappa}(s;\kappa_0)$ as a solution of (2) at the initial value $\kappa_0 = \hat{\kappa}(0)$. The solution must fulfil the boundary condition (6), thus the following non-linear equation is obtained

$$\hat{\kappa}(1,\kappa_0) = 0 \tag{8}$$

which gives κ_0. A good initial guess is usually required to solve (8). The solution can consequently be obtained by iteration. However, the described method is not appropriate if all equilibrium configurations of a cantilever beam with known geometric and material parameters and at a given load are to be obtained. The search for initial values and iterations can be avoided by useing the following algorithm, which converts the two-pointed boundary problem to the problem of initial values (Faulkner et al., 1993; Lipsett et al., 1993):

- at given values ω,λ,v,α the function $\kappa=\hat{\kappa}(1;\kappa_0)$ is tabulated for $\kappa_0\in[-\kappa_{0\max},\kappa_{0\max}]$ so that the problem of initial values (2) is solved with conditions $\phi(0)=-\alpha$ and $\kappa(0)=\kappa_0$;
- from the tabulated value $\kappa=\hat{\kappa}(1;\kappa_0)$ those intervals are eliminated, where $\kappa=\hat{\kappa}(1;\kappa_0)$ changes its sign;
- at the obtained intervals zeros $\hat{\kappa}(1,\kappa_0)=0$ are calculated by means of the secant method;
- for every zero a numerical solution of the problem of initial values (1) and (2) is obtained.

A computer program was written in accord with the described algorithm, which includes the subroutine `rkf45` with the parameters `abstol` = `reltol` $=10^{-9}$ for solving the problem of initial values and the subroutine `zeroin` with the parameter `tol = 0.0` for calculating zeros (Forsythe et al., 1977).

The range of values $\kappa_0\in[-\kappa_{0\max},\kappa_{0\max}]$, where zeros of Eq. (8) are searched for, can be estimated by means of the first integral of the system (2). The estimated values are:

- for $v\frac{\omega^2}{\lambda^2}<1$

$$|\kappa_0| \leqslant \omega\sqrt{2(1+\cos\alpha) - v\frac{\omega^2}{\lambda^2}\sin^2\alpha} \tag{9}$$

- for $v\frac{\omega^2}{\lambda^2}\geqslant 1$

$$|\kappa_0| \leqslant \frac{\lambda}{\sqrt{v}}\left(1+v\frac{\omega^2}{\lambda^2}\cos\alpha\right) \tag{10}$$

It can be noted that the second value can occur only in the case when $v>0$ (i.e., when $EA > GA_s$).

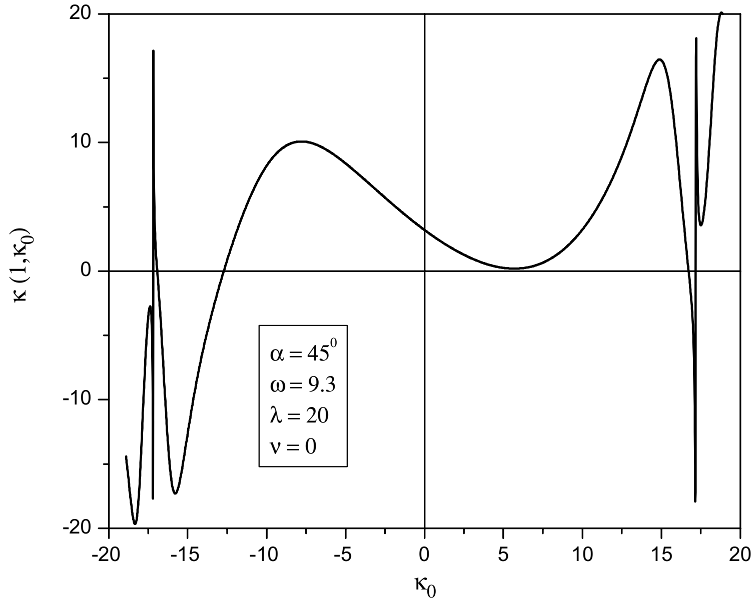

Fig. 2. Bending strain at the free end versus bending strain at the clamped end.

An example of the tabulated values of $\kappa = \hat{\kappa}(1;\kappa_0)$ is shown in Fig. 2. It can be established that the function $\kappa = \hat{\kappa}(1;\kappa_0)$ leaps sharply in the vicinity of $\pm\kappa_{0\,\max}$ (i.e., there are two zeros in the vicinity of that point). For example, in the case of elastica (for the values $\omega = 15$ and $\alpha = 90°$) the zeros lie in the interval of 0.01, while for $\alpha = 0°$ they lie in the interval of 0.027. Via numerical trials the minimum number of intervals, which covers the region $[-\mu_{0\,\max}, \mu_{0\,\max}]$ in such a manner that all zeros are enclosed, was determined as $5.3\exp(\frac{\omega}{1.5})$.

4. Examples

As the first example, the case of elastica for $\alpha = 0$ and $\alpha = \pi/2$ will be analyzed. Because this case implies $1/\lambda = \nu = 0$, the number of possible solutions can be illustrated using the bifurcation diagram showing the function $\kappa_0 = \hat{\kappa}_0(\omega)$, in which the bifurcation points and the number of possible equilibrium shapes at different values ω can be seen. The diagram is shown in Fig. 3 and was constructed using the algorithm by calculating the zeros of $\hat{\kappa}(1,\kappa_0) = 0$ for diferent values of ω.

It can be established that the number of solutions (equilibrium shapes) increases with the load parameter ω. For example, $\omega = 15$ $\alpha = 0$ provides 11 solutions and $\alpha = \pi/2$ provides 9. The corresponding shapes for the examples are shown in Fig. 4. Furthermore, the diagrams show that in the case of $\alpha = 0$ (as opposed to the case of $\alpha = \pi/2$), a trivial solution exists and non-trivial solutions are symmetrical.

Other authors (Navaee and Elling, 1992) have used $\alpha = 45°$, $\omega = 8$ and $\alpha = 45°$, $\omega = 9.325$ for the elastica, obtaining the corresponding equilibrium shapes shown in Fig. 5.

A second example, a test of accuracy of the proposed algorithm by comparing its results to those obtained by Saje, who used the finite element method (Saje, 1991), for a cantilever with $\alpha = 90°$, $F = 10$, $L = 1$, $\mathrm{EA} = 10^{21}$, $\mathrm{EI} = 10$ and various $\mathrm{GA_s}$ was performed. Also an additional comparison with the use of the collocation method implemented in subroutine `colnew` was made (Ascher et al., 1995). A driver pro-

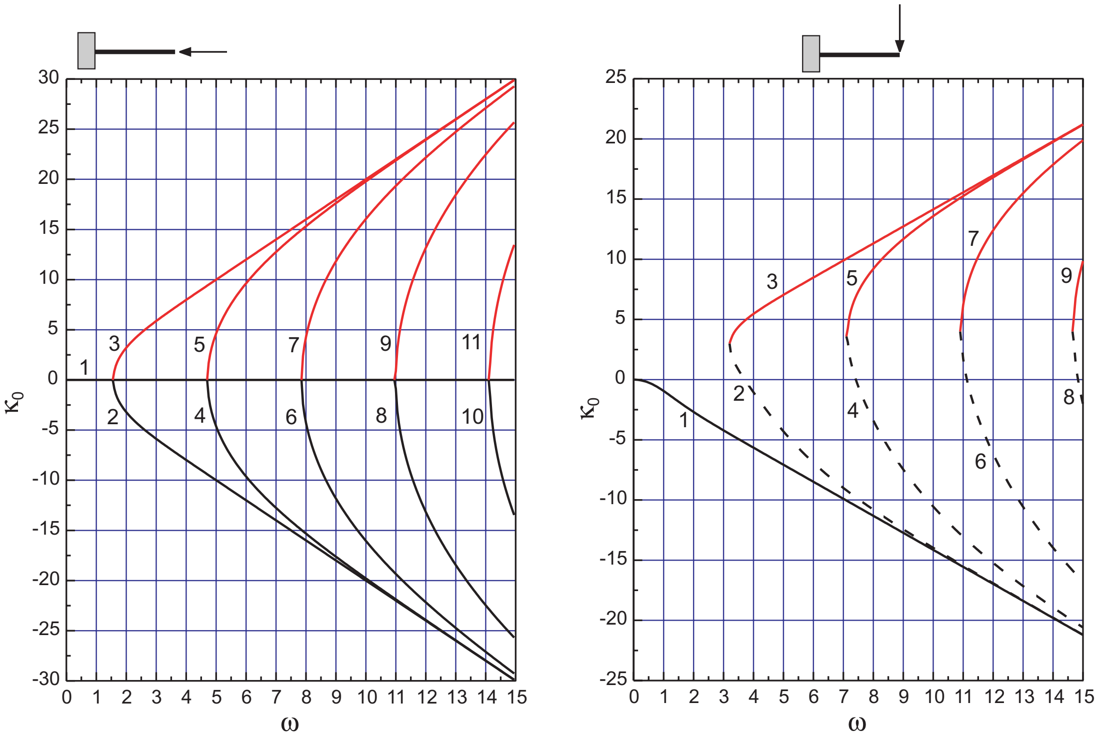

Fig. 3. Bifurcation diagrams for the elastica in the case of $\alpha = 0$ (left) and $\alpha = \pi/2$ (right). The integers correspond to solution branches that give particular equilibrium shapes.

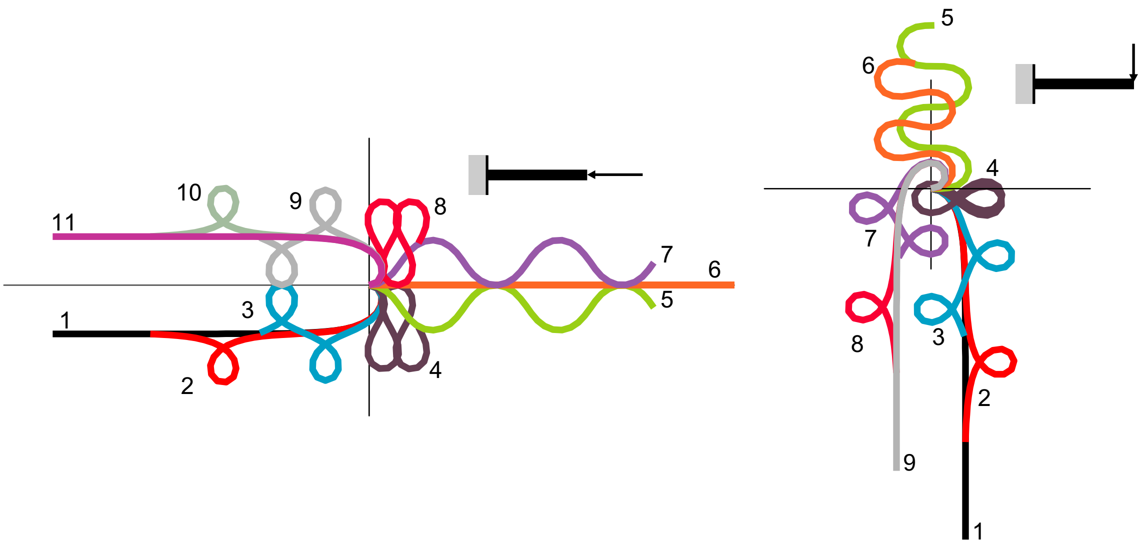

Fig. 4. Equilibrium shapes of an elastica for $\omega = 15$: $\alpha = 0°$, (left), $\alpha = 90°$ (right).

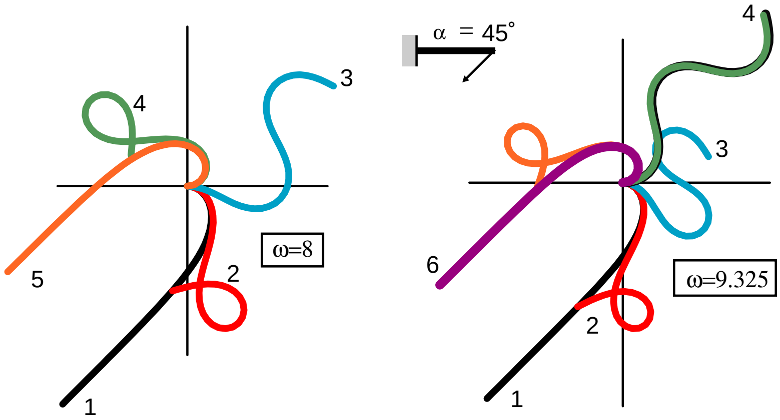

Fig. 5. Equilibrium shapes of an elastica when $\alpha = 45°$: $\omega = 8$ (left) and $\omega = 9.325$ (right).

gram and appropriate subroutines were written for this purpose, which implemented Eqs. (1) and (2) and boundary conditions (5), (6). Since all the cases have only one solution branch, no initial guess subroutine was provided for `colnew`. The error tolerance was set to 10^{-11} for all variables. The comparison of all results is given in Table 1.

The results obtained by `rkf45` and `colnew` are identical to those obtained by Saje up to at least 5 decimal places. A direct comparison of the results produced by `rkf45` and `colnew` show concordance up to 6 decimal places. The discrepancy at the 8th decimal place was observed only in cases $GA_s = 10$ and $GA_s = 5$.

As the third example, a cantilever beam subjected to a horizontal pressure force (i.e., $\alpha = 0$) will be analyzed in detail. As in the case of elastica, the number of equilibrium shapes can be calculated by this algorithm, but the function $\kappa_0 = \hat{\kappa}_0(\omega, \lambda, v)$ should be investigated first. It can be determined that in this case $\phi(0) = 0$; thus on the basis of (7) meaningful solutions are only obtained under the condition

$$\frac{\omega}{\lambda} < \sqrt{\frac{2}{1-v}} \tag{11}$$

Fig. 6 shows graphic representations of areas determined by (11) and the condition $\omega/\lambda > 1\sqrt{v}$, which defines the validity of (10).

Because the discussed boundary problem always has a trivial solution $\phi(s) = \kappa(s) = 0$, its bifurcation points in the vicinity of the trivial solution correspond to the bifurcation points of the linearized problem. The bifurcation points are then defined with the equation

$$v\omega^4/\lambda^2 + \omega^2 - \omega_n^2 = 0 \quad \omega_n = \pi/2 + n\pi \quad (n = 0, 1, 2, \ldots) \tag{12}$$

Table 1

A comparison of the results of calculated components of displacement u and v at the free end of a cantilever for $\alpha = 90°$, $F = 10$, $L = 1$ $EA = 10^{21}$, $EI = 10$ obtained by `rkf45`, `colnew` and Saje (1991)

GA_s	u			v		
	rkf45	colnew	Saje	rkf45	colnew	Saje
5.00E+20	0.05643324	0.05643324	−0.05643	−0.30172077	−0.30172077	0.30172
500	0.06131566	0.06131566	−0.06132	−0.31781387	−0.31781387	0.31781
50	0.10328492	0.10328492	−0.10328	−0.46541330	−0.46541330	0.46541
10	0.25213661	0.25213661	−0.25214	−1.16709588	−1.16709590	1.16710
5	0.37612140	0.37612140	−0.37612	−2.10408747	−2.10408750	2.10409

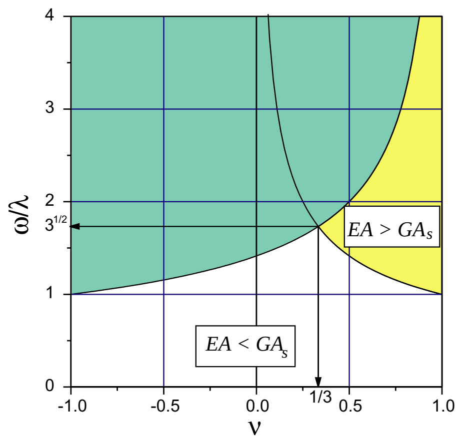

Fig. 6. Intersection of areas $\omega/\lambda > 1/\sqrt{\nu}$, and $\omega/\lambda < \sqrt{2/(1-\nu)}$.

A graphic representation of Eq. (12) for the limit cases $\nu = -1$, $\nu = 1$ and for various values of n (together with shaded areas reflecting inequalities (10) and (11)) is shown in Fig. 7. It can be seen that the behaviour of the beam is highly dependent on parameter ν. For a given value of λ, when $\nu = 1$, it can also be observed that the number of solutions is unlimited; while for $\nu = -1$ the number of solutions is dependent on λ. In general, the turning points of (12) have coordinates $\omega = \sqrt{2}\omega_n$ and $\lambda = 2\omega_n\sqrt{-\nu}$, so values of λ have a lower limit for $\nu < 0$ and at a given n. The least value of λ is in this case $n = 0$, so there are no non-trivial solutions for $\lambda < \pi\sqrt{-\nu}$, while for $\lambda > \pi\sqrt{-\nu}$ the number of solutions increases. Consequently, by taking (11) into consideration for $\nu < 0$, the values of λ are for a given ω limited by $\lambda > \max(\pi\sqrt{-\nu}, \omega\sqrt{\frac{1-\nu}{2}})$. For $\nu > 0$ (12) has no turning points, so the values of λ are for a given ω bounded only by (11); i.e., one has $\lambda > \omega\sqrt{\frac{1-\nu}{2}}$.

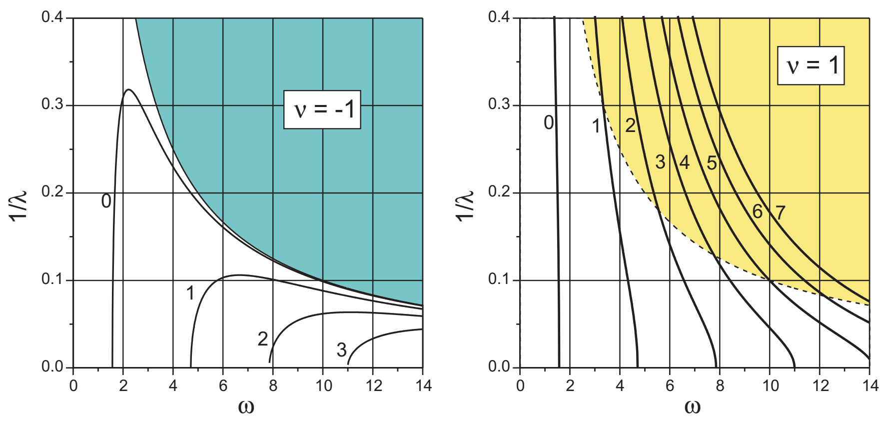

Fig. 7. Graphic representation of the function $\nu\omega^4/\lambda^2 + \omega^2 - (\pi/2 + n\pi)^2 = 0$ for $\nu = -1$ (left) and $\nu = 1$ (right), for various n. The shaded areas correspond to the regions in Fig. 4.

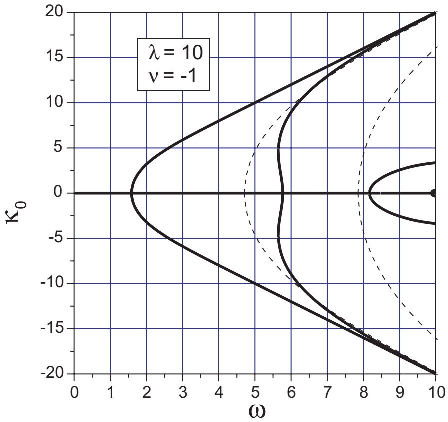

Fig. 8. Bifurcation diagram for $\lambda = 10$, $\nu = -1$ (bold curve) and for the elastica (dash curve).

Before proceeding to specific examples, the point should be made that Eq. (12) does not present all the bifurcation points. For example, in Fig. 8, which represents the bifurcation diagram for $\lambda = 10$ and $\nu = -1$ two additional bifurcation points with coordinates (5.6478 ± 4.3988) exist.

The first example has the parameters $\omega = 5.7$, $\lambda = 10$, and is shown in Fig. 9. In the case $\nu = -1$ (according to the bifurcation diagram in Fig. 8) seven equilibrium shapes are obtained, while for $\nu = 0$ five equilibrium shapes occur.

The second example has the parameters $\lambda = 5, \nu = 1$ and defines a cantilever beam that allows no extension strain. Its equilibrium shapes are shown in Figs. 10–12. For $\omega = 4$ five, for $\omega = 6$ seven and for $\omega = 9$ thirteen equilibrium shapes are obtained.

For the purpose of numerical comparison calculated values of κ_0 and calculated values of variables at the free end for the first example (left example in Fig. 9, Table 2) and for the second example (Fig. 12, Table 3) are given. Because the solutions are symmetrical, only the first four solutions for the first example and the first seven for the second example are given. The variable s^+ in the tables represents the length of the deformed beam, which is obtained with the integration of equation

$$\frac{\mathrm{d}s^+}{\mathrm{d}s} = \sqrt{(1+\varepsilon)^2 + \gamma^2} \quad s^+(0) = 0 \tag{13}$$

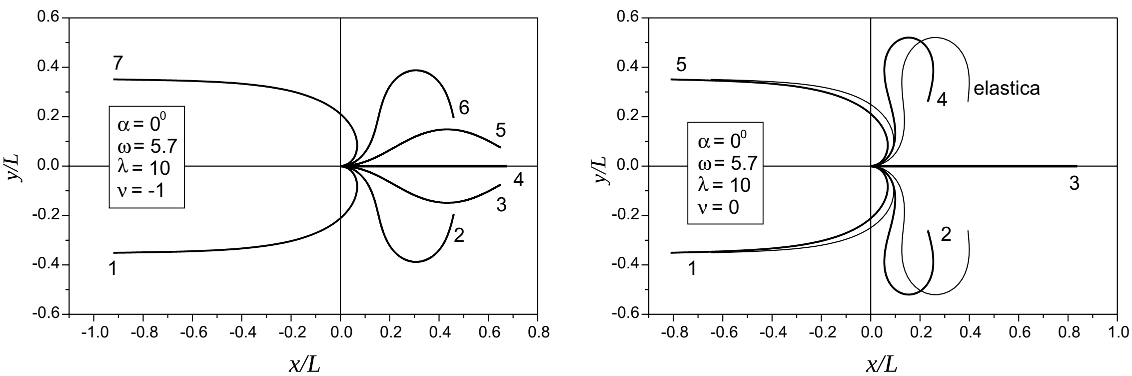

Fig. 9. Equilibrium shapes of a cantilever beam for $\alpha = 0°$, $\omega = 5.7$, $\lambda = 10$: $\nu = -1$ (left), $\nu = 0$ (right).

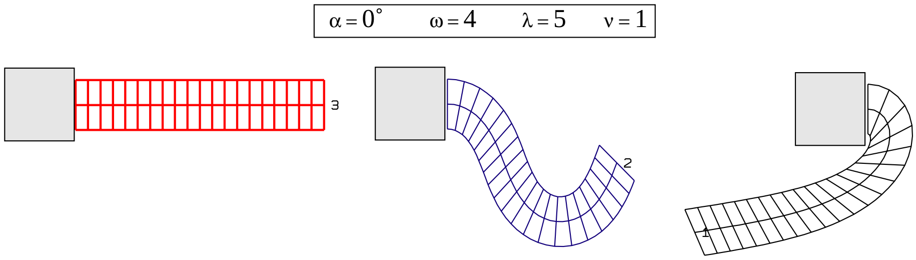

Fig. 10. Equilibrium shapes 1, 2 and 3 of a cantilever beam for $\alpha = 0°$, $\omega = 4$, $\lambda = 5$, $\nu = 1$.

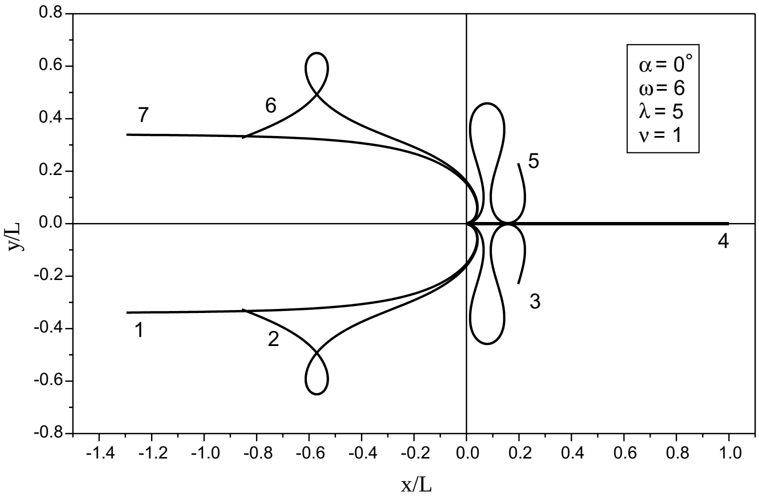

Fig. 11. Equilibrium shapes of a cantilever beam for $\alpha = 0°$, $\omega = 6$, $\lambda = 5$, $\nu = 1$.

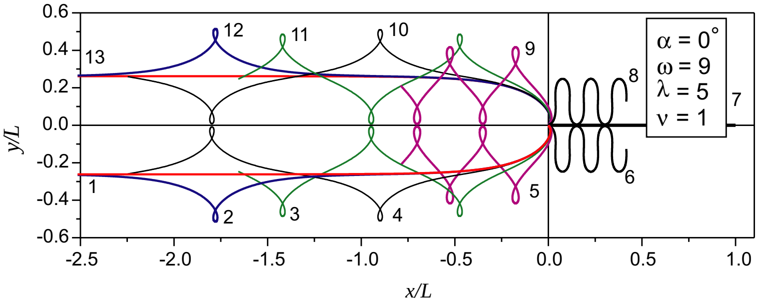

Fig. 12. Equilibrium shapes of a cantilever beam for $\alpha = 0°$, $\omega = 9$, $\lambda = 5$, $\nu = 1$.

It can be noted that the values of κ_0 in the first and second row in Table 3 are very close and that the value of $\hat{\kappa}(1;\kappa_0)$ in the first row is accurate only at two decimal places. These values correspond to shapes 1 and 2 in Fig. 12.

Table 2
The calculated values of variables for $\alpha = 0°$, $\omega = 5.7$, $\lambda = 10$, $v = -1$

	κ_0	x_1	y_1	ϕ_1	$\hat{\kappa}(1;\kappa_0)$	s^+	$1+\varepsilon_1$
1	−11.399680	−0.920963	−0.350867	−3.128565	0.000001	1.216300	1.324872
2	−6.307238	0.459807	−0.194129	1.334342	0.000000	0.804732	0.923890
3	−2.415322	0.650371	−0.074340	0.513525	0.000000	0.696150	0.717006
4	0.000000	0.675100	0.000000	0.000000	0.000000	0.675100	0.675100

Table 3
The calculated values of variables for $\alpha = 0°$, $\omega = 9$, $\lambda = 5$, $v = 1$

	κ_0	x_1	y_1	ϕ_1	$\hat{\kappa}(1;\kappa_0)$	s^+	$1+\varepsilon_1$
1	−21.200000	−3.049771	−0.261749	−1.884455	0.001633	3.185312	1.000000
2	−21.197194	−2.668575	−0.261694	1.862258	−0.000001	3.075509	1.000000
3	−21.021542	−2.247130	−0.259525	−1.710450	0.000000	2.943451	1.000000
4	−20.005497	−1.656486	−0.246981	1.446047	0.000000	2.717856	1.000000
5	−17.181012	−0.789141	−0.212111	−1.095035	0.000000	2.319023	1.000000
6	−10.210749	0.415995	−0.126059	0.576800	0.000000	1.579974	1.000000
7	0.000000	1.000000	0.000000	0.000000	0.000000	1.000000	1.000000

5. Conclusion

The results show that the proposed numerical method is suitable for the determination of all equilibrium configurations of a cantilever beam by means of finite-strain beam theory. It is shown how the introduced material parameters λ, v and the load parameter ω influence the number of equilibrium configurations. Unlike in the case of elastica, for which the number of equilibrium shapes is dependent on ω, it is demonstrated that in the case of finite strain for $v < 0$ values λ exist, for which the beam has only a single (output) shape irrespective of ω. The numerical results can be used as comparative values when testing the accuracy of various numerical methods in elasticity.

References

Antman, S.S., 1995. Nonlinear Problems of Elasticity. Springer-Verlag, Berlin.

Ascher, U.M., Mattheij, R.M.M., Russell, R.D., 1995. Numerical Solution of Boundary Value Problems for Ordinary Differential Equations. SIAM, Philadelphia.

Faulkner, M.G., Lipsett, A.W., Tam, V., 1993. On the use of a segmental shooting technique for multiple solutions of planar elastic problems. Computer Methods in Applied Mechanics and Engineering 110, 221–236.

Forsythe, G.E., Malcolm, M.A., Moler, C.B., 1977. Computer Methods for Mathematical Computations. Prentice-Hall, New Jersey.

Landau, L.D., Lifshitz, E.M., 1986. Theory of Elasticity. Pergamon Press, New York.

Lipsett, A.W., Faulkner, M.G., Tam, V., 1993. Multiple solutions for inextensible arches. Transactions of the CSME 17 (1), 1–15.

Love, A.E.H., 1944. A Treatise on the Mathematical Theory of Elasticity. Dover Publication, New York.

Navaee, S., Elling, R.E., 1992. Equilibrium configurations of cantilever beams subjected to inclined end loads. Transactions of ASME, Journal of Applied Mechanics 59, 572–579.

Pai, P.F., Palazotto, A.N., 1996. Large-deformation analysis of flexible beams. International Journal of Solids and Structures 33 (9), 1335–1353.

Reissner, E., 1972. On one-dimensional finite-strain beam theory: the plane problem. Journal of Applied Mathematics and Physics (ZAMP) 23, 795–804.

Saje, M., 1990. A variational principle for finite planar deformation of straight slender elastic beams. International Journal of Solids and Structures 26 (8), 887–900.

Saje, M., 1991. Finite element formulation of finite planar deformation of curved elastic beams. Computers and Structures 39 (3/4), 327–337.